BALASUBRAMANIAM A. S. & WAHEED-UDDIN (1977). *Géotechnique* 27, No. 1, 75–92.

Deformation characteristics of weathered Bangkok Clay in triaxial extension

A. S. BALASUBRAMANIAM, BSc, PhD, MICE, MASCE, FGS*
and WAHEED-UDDIN, BSc, MEng†

The deformation characteristics of weathered Bangkok Clay is studied in detail by carrying out two series of strain controlled undrained triaxial tests under extension conditions. Undisturbed samples of weathered clay were taken at a depth of 2·5 m to 3 m from Bangpli (Nong Ngoo Hao), a site situated 28 km southeast from Bangkok, Thailand. Both series of tests were carried out on isotropically consolidated samples. However, Series I corresponded to the case wherein the axial stress was reduced while the lateral stress was maintained constant. In the second series of tests, the axial stress was kept constant and the laterial stress was increased. The stress–strain behaviour and strength characteristics from both types are presented and discussed.

Les caractéristiques de déformation de l'argile altérée de Bangkok sont étudiées en détail en effectuant deux séries d'essais triaxiaux non-drainés à déformation imposée dans des conditions d'extension. Des échantillons intacts d'argile ont été prélevés, à une profondeur de 2·5 m à 3 m, à Bangpli (Nong Ngoo Hao), un chantier situé à 28 km au sud-est de Bangkok, Thaïlande. Les deux séries d'essais on été effectuées sur des échantillons consolidés isotropiquements. Cependant, la série I correspond au cas où la tension axiale est réduite pendant que la tension latérale est maintenue constante. Dans la deuxième série d'essais, la tension axiale a été gardée constante et la tension latérale augmentée. Le comportement contrainte–déformation et les caractéristiques de résistance des deux types d'essais sont présentés et discutés.

INTRODUCTION

Triaxial compression tests have commonly been carried out on Bangkok Clays to investigate the shear strength characteristics and the stress–strain behaviour under various applied stress paths. For some investigations, however, such as the heave of the bottom of an excavation, or in the design of sheet-pile walls, it is essential to have a knowledge of the deformation characteristics under extension conditions. The work presented in this Paper forms the first attempt to carry out a comprehensive series of extension tests on weathered Bangkok Clay. Previous work carried out on triaxial extension tests in clays include those of Parry (1960), Wu *et al.* (1963), Shibata and Karube (1965), Vaid and Campanella (1974) and Parry and Nadarajah (1974).

Moh *et al.* (1969) were the first to carry out a study on the shear strength characteristics of Bangkok Clay as observed from consolidated undrained triaxial compression tests. Since then, a considerable amount of work on the undrained shear strength of weathered Bangkok Clay has been carried out by several research workers (see Chang, 1974; Wang, 1974; etc.).

Weathered Bangkok Clay has been found to behave as an overconsolidated clay (see Moh *et al.*, 1969) at low consolidation pressures. This apparent overconsolidation is thought to be due to weathering effects and seasonal fluctuations in the ground water table. In this study a wide range of pre-shear consolidation pressures have been selected to cover both the overconsolidation and the normally consolidated range.

Discussion on this Paper closes 1 June, 1977. For further details see inside back cover.

* Associate Professor of Geotechnical Engineering, Asian Institute of Technology, Bangkok.
† Resident Engineer, NACO, Jeddah.

NOTATION

u	pore pressure	w	water content
A	pore pressure coefficient	dv	incremental volumetric strain
e	voids ratio	V_0	volume of sample at the end of consolidation
l_0	height of sample at the end of consolidation	V	current volume
l	current height of sample	$\sigma'_1, \sigma'_2, \sigma'_3$	principal effective compressive stress
M	slope of critical state line in (q, p) plot	$\eta = q/p$	stress ratio
p	mean normal stress	$d\epsilon_1, d\epsilon_2, d\epsilon_3$	incremental principal strain
p_0	pre-shear consolidation stress	$d\epsilon$	incremental shear strain
q	deviator stress	Φ	angle of internal friction
S	degree of saturation	Suffix f refers to failure condition	

Notable contributions on the stress–strain behaviour of soft clay have recently been made by Roscoe and Poorooshasb (1963), Roscoe *et al.* (1963), Roscoe and Burland (1968) and Schofield and Wroth (1968). The work presented in this Paper would form a useful bulk of information for the development of a successful stress–strain theory for weathered Bangkok Clay.

DEFINITIONS

The stress parameters p and q are defined by

$$p = (\sigma'_1 + 2\sigma'_3)/3$$
$$q = (\sigma'_1 - \sigma'_3)$$

where σ'_1, σ'_2 and σ'_3 are the principal effective compressive stresses, and $\sigma'_2 = \sigma'_3$ under the triaxial stress system. Similarly, the incremental strain parameters dv and $d\epsilon$ are given by

$$dv = d\epsilon_1 + 2d\epsilon_3$$
$$d\epsilon = 2(d\epsilon_1 - d\epsilon_3)/3$$

where $d\epsilon_1$, $d\epsilon_2$ and $d\epsilon_3$ are the principal incremental compressive strains and $d\epsilon_2$ is equal to $d\epsilon_3$ under the triaxial stress system. The stress ratio η is equal to q/p. The axial and volumetric strains are defined as

$$\epsilon_1 = \log (l_0/l) \quad \text{and} \quad v = \log (V_0/V)$$

when l_0 and V_0 are the initial height and volume of the sample respectively; l and V correspond to current values.

DESCRIPTION OF WEATHERED BANGKOK CLAY

The subsoil profile at Bangpli is essentially the same as that already presented for the area north of Bangkok (Muktabhant *et al.*, 1967; Moh *et al.*, 1969). The weathered zone is about 4 m thick. Observations during the sampling indicate a marked effect of weathering process in this zone. In the upper part the soil was found to be dark grey in colour, and light brown horizontal silt seams were observed at different depths in the upper 2 metre thickness. Small holes were also found in this portion, probably created by earthworms or decayed roots. Between 2·0 m and 2·5 m, a layer of light grey clay was noted having traces of dark coloured

decayed organic matter. Below a depth of 2·5 m, the soil became more uniform in colour; the holes were no longer apparent. A few samples obtained from depths of 2·5 m and 3·0 m contained traces of silt seams and lenses of fine sand.

The index properties of the clay are as follows

Natural water content, %	133 ± 5	Soluble salt content, g/litre	7·0
Natural void ratio	$3{\cdot}86 \pm 0{\cdot}15$	Organic matter, %	4
Degree of saturation, %	95 ± 2	pH	8·5
Specific gravity	2·73	*Grain size distribution*	
Liquid limit, %	123 ± 2	Sand, %	7·5
Plastic limit, %	41 ± 2	Silt, %	23·5
Plasticity index	82 ± 4	Clay, %	69
Dry density (lb/ft^3)	36 ± 2	Colour	Dark grey

SAMPLE PREPARATION AND TESTING PROCEDURE

Soil samples were taken using a boring rig from depths of 2·5 to 3·0 m; 25·4 mm diameter and long thin-walled sample tubes were used for taking undisturbed samples.

After extruding the samples from the 25·4 mm dia. Shelby tubes, they were cut into pieces, covered with wax and paraffin and were stored in the humidity-controlled room. During the testing phase each piece of sample stored in the moist room was taken out, paraffin and wax carefully removed and trimmed down to the required size. Two porous stones were placed one at each end of the sample. Also Whatman No. 40 filter paper side drains were placed along the circumference of the sample. The sample was then enclosed within two rubber membranes which were separated by a thin coating of silicone grease. The upper and lower ends of the rubber membrane were sealed against the top cap and the pedestal respectively, by hard Gaco 'O' ring seals. The chamber surrounding the sample was then filled with silicone oil.

For all test series, the samples were consolidated isotropically at various consolidation pressures. The consolidation was carried out against an elevated pore pressure to ensure complete saturation of the sample. A back pressure of 207 kN/m^2 was applied which has been found usually sufficient to dissolve all the air. The volume change of the sample was measured at various intervals of time until all the excess pore pressure was dissipated. Depending on the consolidation pressure, the duration for full dissipation of pore pressure varied from 2 to 5 days.

A systematic test programme was designed to investigate the stress–strain behaviour and strength characteristics of weathered Bangkok Clay under extension condition when tested in the triaxial apparatus. Four series of triaxial extension tests were carried out. The designations of the test series are as given below:

(*a*) CIUE-I Consolidated undrained triaxial extension test on isotropically consolidated samples (under unloading path); i.e. keeping the cell pressure constant and reducing the axial stress.

(*b*) CIUE-II Consolidated undrained triaxial extension test on isotropically consolidated samples (under loading path); i.e. keeping the axial stress constant and increasing the cell pressure.

(*c*) CIDE Consolidated drained triaxial extension test on isotropically consolidated samples under unloading path.

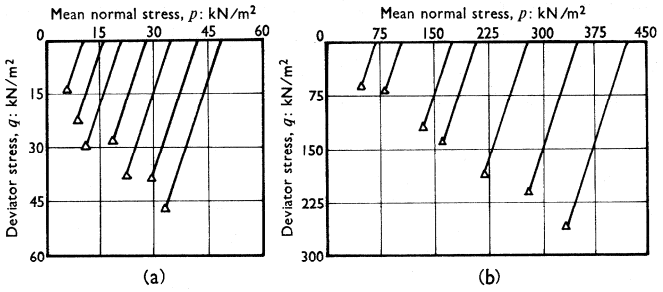

Fig. 1. Applied stress paths on specimens sheared in Series CIUE-I tests: (a) $p_0 < 69$ kN/m²; (b) $p_0 \geq 69$ kN/m²

(*d*) CIEU-*p* Consolidated undrained triaxial extension test on isotropically consolidated samples having the same maximum consolidation pressure of 414 kN/m² and then swelled to different overconsolidation ratios.

All the samples for the triaxial extension tests were sheared under strain controlled conditions. Only the results of test series CIUE-I and CIUE-II will be presented here.

RESULTS OF TEST SERIES CIUE-I

Table 1 summarizes the details of 14 undrained triaxial extension tests in Series CIUE-I. These details include the water contents, void ratios, degree of saturation and dry density for all the natural samples prior to and at the end of isotropic consolidation. The isotropic consolidation stress varied from 10·4 kN/m² to 414 kN/m².

A critical pressure has been found to exist in weathered Bangkok Clay which separates the stress conditions for which the samples behave as normally consolidated from those for which the behaviour corresponded to overconsolidated samples. The behaviour of the clay under undrained triaxial condition corresponds to normally consolidated samples for all values of consolidation pressures higher than this critical pressure. For samples consolidated at stress levels below the critical pressure, the behaviour under undrained compression conditions was similar to that for overconsolidated clay.

Table 1. Data associated with specimens of CIUE-I series of tests

Test No.	Consolidation pressure (p_0), kN/m²	Initial condition				At the end of isotropic consolidation			
		w%	e	S%	$1000 \times \gamma_d$ kg/m³	w%	e	S%	$1000 \times \gamma_d$ kg/m³
1	10·4	138·0	4·0	94·4	0·550	138·9	3·79	100·0	0·565
2	15·9	130·0	3·77	94·2	0·570	129·1	3·52	100·0	0·576
3	20·7	138·5	4·02	94·0	0·545	136·2	3·72	100·0	0·559
4	27·6	130·0	3·81	93·2	0·569	125·4	3·42	100·0	0·584
5	34·5	140·0	4·10	93·2	0·536	133·1	3·63	100·0	0·559
6	41·4	128·0	3·53	99·1	0·604	118·3	3·23	100·0	0·655
7	48·3	133·2	3·82	95·1	0·567	111·8	3·05	100·0	0·642
8	69·0	128·0	3·56	98·2	0·600	98·5	2·69	100·0	0·727
9	103·5	131·5	3·74	96·0	0·577	88·5	2·42	100·0	0·751
10	172·5	130·0	3·78	94·0	0·572	80·7	2·20	100·0	0·809
11	207·0	129·0	3·77	93·4	0·573	80·6	2·20	100·0	0·862
12	276·0	137·0	4·01	93·2	0·546	71·6	1·95	100·0	0·887
13	345·0	137·5	3·96	94·7	0·551	69·7	1·89	100·0	0·922
14	414·0	131·0	3·74	95·6	0·578	65·3	1·78	100·0	0·980

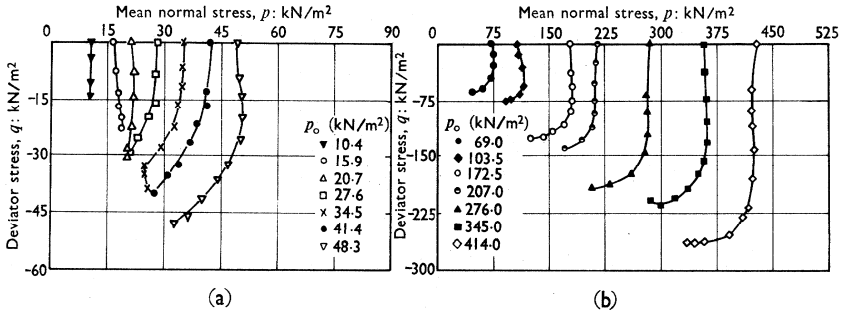

Fig. 2. Effective stress paths followed by specimens in Series CIUE-I tests: (a) $p_0 < 69$ kN/m²; (b) $p_0 \geq 69$ kN/m²

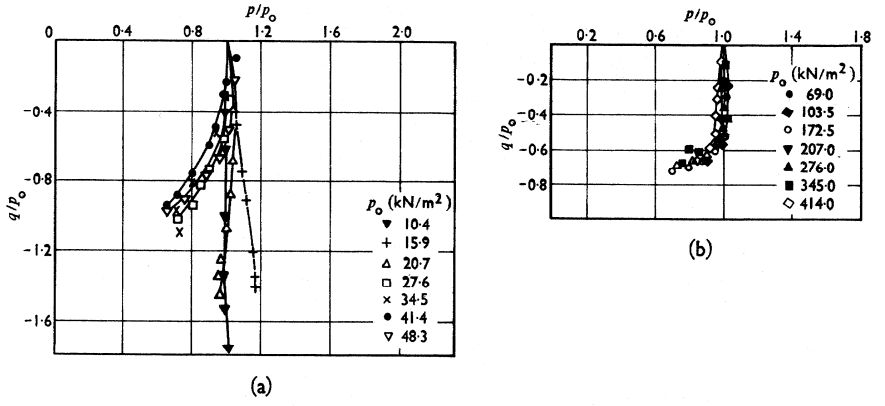

Fig. 3. Normalized effective stress paths: (a) $p_0 < 69$ kN/m²; (b) $p_0 \geq 69$ kN/m²

It is, therefore, thought to be logical to present the data from Series CIUE-I tests in two parts. First, the data will be presented for all the tests in which the consolidation pressures were less than 69 kN/m² and therefore correspond to stress conditions below the critical pressure level. The second part will contain all the data from tests in which the samples were consolidated to pressures higher than the critical pressure.

Stress paths

The applied stress paths of the specimens having a slope $|dq/dp|$ of 3 are shown in Fig. 1. The effective stress paths during shear of the samples consolidated to pre-shear consolidation pressures less than 69 kN/m² are shown in Fig. 2(a). The shape and position of the effective stress paths in this plot will depend on the magnitude of the pre-shear consolidation pressure. It is noted that the initial portion of the effective stress paths for all the samples are nearly parallel to the q-axis. For all the tests at higher consolidation pressures (41·4 or 48·3 kN/m²) initially the stress paths are nearly parallel to q-axis and thereafter they gradually deviate with decreasing p. These stress paths are similar to those followed by lightly overconsolidated clays.

The effective stress paths of the samples at low consolidation pressures (e.g. at 10·4 and 15·9 kN/m²) continue to be parallel to the q-axis until failure. However, for the specimens sheared from pre-shear consolidation pressures of 20·7 and 27·6 kN/m², the effective stress paths deviate towards the origin with decreasing p.

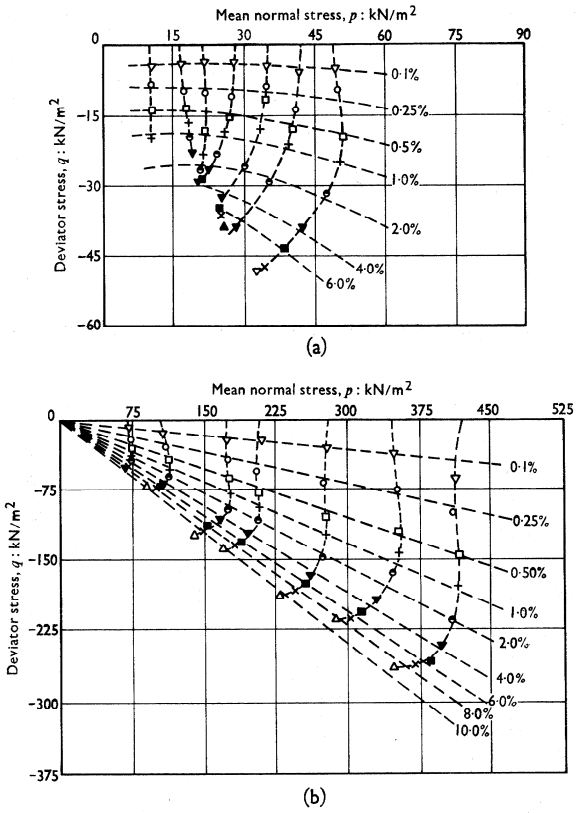

Fig. 4. Shear strain contours superimposed on effective stress paths: (a) $p_0 < 69$ kN/m^2; (b) $p_0 \geq 69$ kN/m^2

Figure 2(b) illustrates the effective stress paths for the samples sheared under undrained condition from the higher pre-shear consolidation pressures. Even for these specimens, the initial portion of the stress paths are found to be nearly parallel to the q-axis. This effect may be due to the development of negative pore pressure in the sample. As soon as the excess pore pressure increases, the mean normal stress will begin to decrease. Then the effective stress paths tend to become convex towards the origin. Another characteristic of these paths is that all of them are geometrically similar. It has been observed that the stress paths followed by samples of normally consolidated clay are similar in shape.

The effective stress paths are normalized by dividing the deviator stress q and the mean normal stress p by the respective consolidation pressure (p_0). For a normally consolidated clay a unique curve is achieved on the normalized plot of the effective stress paths (see Balasubramaniam, 1974). For samples below 69 kN/m^2 consolidation pressure, the normalized effective stress paths have been plotted in Fig. 3(a). No unique curve exists for these specimens in the normalized plot, however, but the shape and position of the normalized effective stress paths are found to depend on the consolidation pressures.

Figure 3(b) shows the normalized effective stress paths for the samples at higher consolidation pressures. Within the limits of experimental errors, the normalized effective stress paths seem to form a unique curve at higher consolidation pressure corresponding to the normally consolidated state.

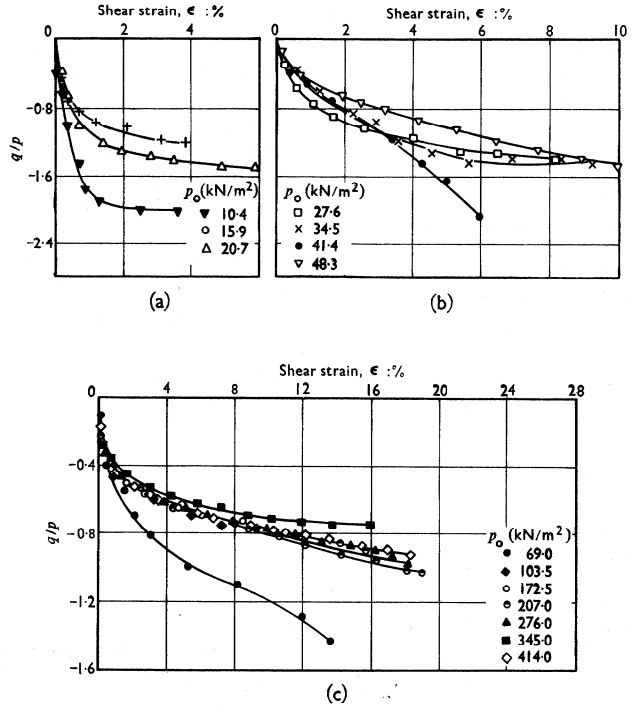

Fig. 5. Stress ratio–shear strain relationship: (a) $p_0 < 20{\cdot}7$ kN/m²; (b) $20{\cdot}7 < p_0 < 69$ kN/m²; (c) $p_0 \geq 69$ kN/m²

Shear strain contours

Figure 4(a) shows a family of equal shear strain contours superimposed on the undrained effective stress paths of Fig. 2(a). These shear strain contours have been plotted at convenient intervals of strain. If the samples are normally consolidated, the equal shear strain contours have been found to be straight lines passing through the origin (see Roscoe and Poorooshasb, 1963). But for the overconsolidated samples, the equal shear strain contours do not pass through the origin (see Wroth and Loudon, 1967). In the apparent overconsolidated range, the trend followed by the equal shear strain contours show no indication of passing through the origin. At lower strain levels, the contours form curved lines which tend to be slightly concave to the p-axis. But these contours are nearly parallel to each other. This trend indicates that the shear strain depends largely on the increment of the deviator stress rather than on any change in the effective mean normal stress. At higher strains, the shear strain contours tend to become more curved as one moves from lower to higher consolidation pressures. Equal shear strain contours for samples in the normally consolidated range have been superimposed on the effective stress paths in (q, p) plot in Fig. 4(b). The shear strain contours on this plot form straight lines which converge at the origin. This finding is the same as that reported by other investigators for normally consolidated clay (see Roscoe and Poorooshasb, 1963). The Author's results, therefore, indicate that the shear strains in these samples depend solely on the effective stress ratio q/p.

Stress ratio (q/p) against shear strain relationship

For the samples in the apparent overconsolidated range, plots of the stress ratio (q/p) against shear strain were shown in Figs 5(a) and (b). It is evident that the stress ratio against shear strain relationship is dependent on the consolidation pressures. Fig. 5(c) shows the stress

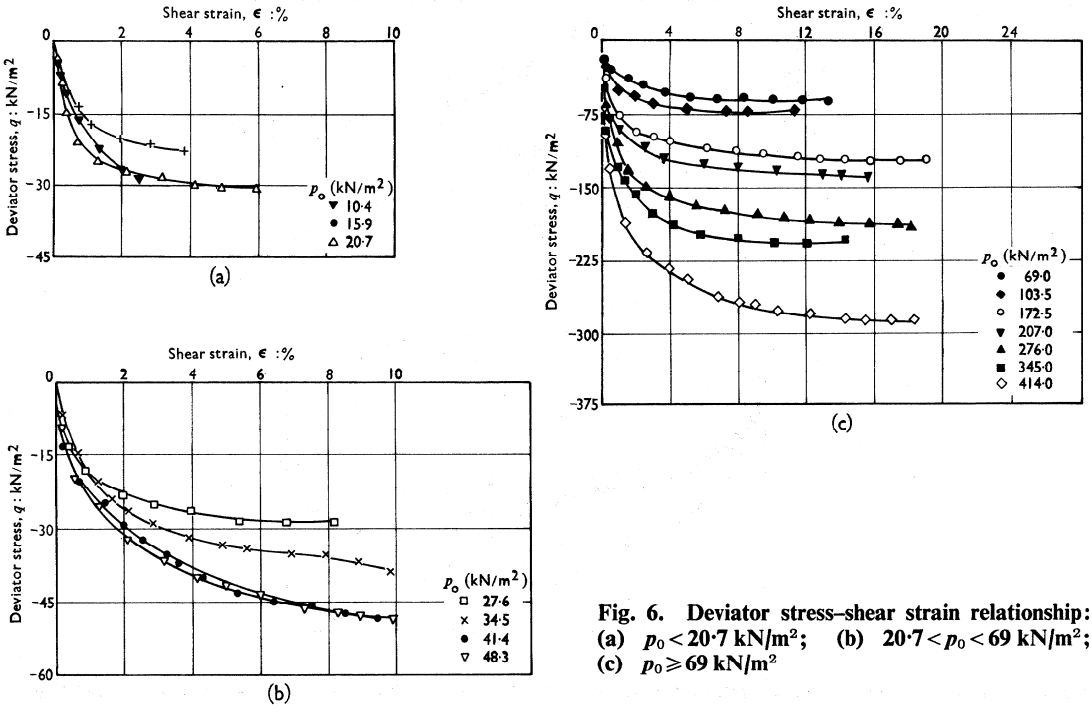

Fig. 6. Deviator stress–shear strain relationship: (a) $p_0 < 20{\cdot}7$ kN/m²; (b) $20{\cdot}7 < p_0 < 69$ kN/m²; (c) $p_0 \geq 69$ kN/m²

ratio (q/p) plotted against shear strain for samples at higher consolidation pressures. It is apparent from Fig. 5(c) that for samples at consolidation pressures higher than 69 kN/m² the q/p against shear strain relationships form an almost unique curve. This finding is typical for normally consolidated samples (see Balasubramaniam, 1973).

Deviator stress axial strain relationship

Figures 6(a) to (c) illustrate the deviator stress–shear strain relationships for all the samples included in Series CIUE-I. Figs 6(a) and (b) correspond to the samples tested at consolidation pressures less than 69 kN/m² and Fig. 6(c) presents the relationship for samples tested at consolidation pressures higher than 69 kN/m². In these figures, at any particular strain, the deviator stress was found to increase with increase in pre-shear consolidation pressure of the samples. Also, the deviator stress–strain relationships shown in Figs 6(a) and (b) do not seem to indicate any well-defined peaks as those generally observed in samples of weathered clay tested in compression with consolidation pressures well below the critical pressure. Perhaps this phenomenon could be attributed to the inherent instability that develops in the sample under extension condition. During extension, the sample tends to form a neck (having a much smaller area) and therefore an increase in deformation will make the sample weak and unstable. However, during compression the area of the sample increases and therefore a tendency for such instability does not exist unless an eccentricity in the axial load results during shearing. Another interesting phenomenon observed is that for samples consolidated at low pressures, the modulus of the stress–strain curve was found to be high. For example, for the samples tested at 20·7 kN/m² consolidation pressure, 75% of the peak deviator stress was reached at about 1% of shear strain. However, for the sample sheared from 34·5 kN/m² consolidation pressure, the corresponding valuc of the shear strain was about 2%. Beyond

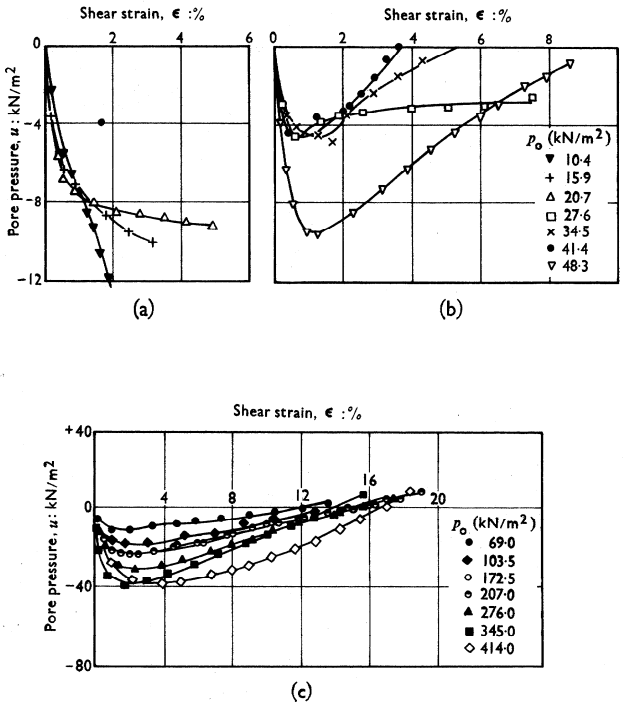

Fig. 7. Pore pressure–shear strain relationship: (a) $p_o < 20{\cdot}7$ kN/m²; (b) $20{\cdot}7 < p_o < 69$ kN/m²; (c) $p_o \geq 69$ kN/m²

a value of 75% of the deviator stress, the ratio of the increase in deviator stress with incremental strain is low and the stress–strain curves become more or less parallel to the strain axis. The magnitude of the shear strain at which peak deviator stress occurred seems to be dependent on the pre-shear consolidation pressure. For the sample consolidated at 20·7 kN/m², the maximum deviator stress was attained at about 6% of shear strain, whereas the maximum deviator stress occurred at about 10% of shear strain for the sample consolidated at 48·3 kN/m².

Figure 6(c) shows plots of deviator stress against shear strain for the samples tested at higher consolidation stresses. In all these tests the deviator stress increased rapidly in the initial stage. But in contrast to samples at low consolidation pressure, the rate of increase of deviator stress in this series of tests was lower and was nearly independent of the consolidation pressure.

Excess pore pressure against shear strain relationship

Figures 7(a) and (b) show plots of excess pore pressure against shear strain for the samples tested from consolidation pressures less than 69 kN/m². At very low consolidation pressures 10·4, 15·9, 20·7 kN/m² the samples develop large negative pore pressure which continues to decrease with increasing strain. Similar results were found by Parry (1960) from triaxial undrained extension tests on heavily overconsolidated samples of Weald Clay and London Clay. For samples consolidated to higher stresses (27·6, 34·5, 41·4, 48·3 kN/m²), the excess pore pressure strain relationships show peak negative values, and the pore pressures then tend to increase with increase in shear strain. At failure, the excess pore pressures were found to be almost zero for these samples.

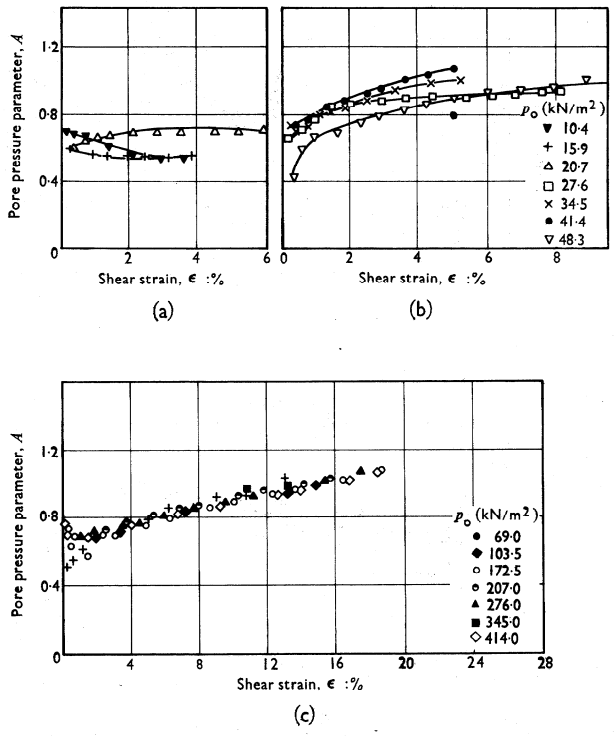

Fig. 8. Pore pressure coefficient A–shear strain relationship: (a) $p_0 < 20{\cdot}7$ kN/m²; (b) $20{\cdot}7 < p_0 < 69$ kN/m²; (c) $p_0 \geq 69$ kN/m²

For the samples consolidated to stresses higher than 69 kN/m², the excess pore pressures have been plotted in Fig. 7(c) as a function of shear strain. All these samples which were in the normally consolidated state developed negative pore pressures at low strain levels, and then showed a gradual increase in the pore pressure until near failure, when the pore pressures in these samples became positive. The maximum values of the negative pore pressures vary with respect to the consolidation pressures. The sample sheared from higher consolidation pressure shows a higher value of the maximum negative pore pressure. The development of negative pore pressure in these triaxial extension tests is due to the unloading condition imposed on the sample during shear.

Pore pressure coefficient A against shear strain relationship

Figures 8(a) and (b) illustrate the variations of the pore pressure coefficient A with respect to shear strain for samples sheared from consolidation pressures corresponding to the apparent overconsolidated state. For all these samples values of A initially lie between 0·6 and 0·7. Variation of A with respect to strain depends on the corresponding consolidation pressure. For very low consolidation pressure (e.g. 10·4 kN/m²), the value of A decreases with respect to strain to 0·5. At higher consolidation pressures the value of A increases with strain. At failure, the value of A varies with respect to consolidation pressure and it reaches a minimum for the lowest consolidation pressure.

Figure 8(c) shows the pore pressure coefficient A against shear strain relationship for samples at pre-shear stresses at and above 69 kN/m². For all these samples which are in the normally

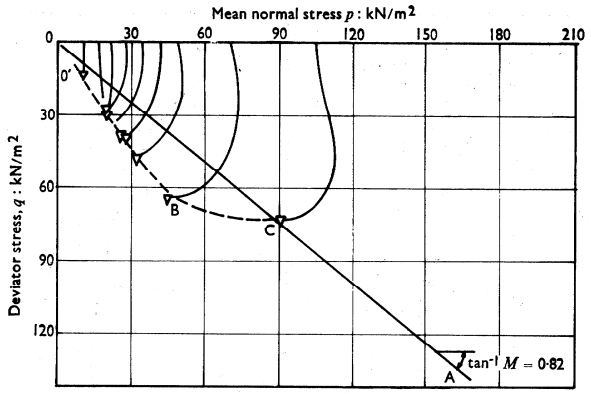

Fig. 9. End points of specimens in (q, p) plot, $p_0 < 69$ kN/m^2

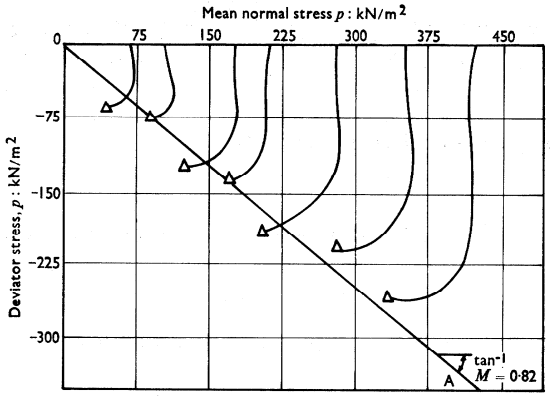

Fig. 10. End points of specimens in (q, p) plot, $p_0 \geq 69$ kN/m^2

consolidated state, the value of A is initially near 0·7 and the variation of A with respect to strain is unique. The value of A at failure (A_f) for these samples is about one.

Shear strength characteristics

The data associated with the CIUE-I series of tests conducted on specimens of weathered clay consolidated to 10·4, 15·9, 20·7, 27·6, 34·5, 41·4, 48·3, 69 and 104 kN/m^2 isotropic stresses are presented in Fig. 9. The specimens were sheared under undrained unloading conditions.

In Fig. 9, the end points of the specimens based on $(\bar{\sigma}_3/\bar{\sigma}_1)_{max}$ criterion are shown in (q, p) plot. The effective stress paths followed by the specimens are also shown. In this figure the line OA corresponds to the end points of the samples sheared to failure from pre-shear consolidation pressures of 103·5, 172·5, 207, 276, 345 and 414 kN/m^2. Thus the line OA in the (q, p) plot would correspond to the projection of the critical state line for extension tests. Also, in the same figure, the broken line OBC corresponds to the failure envelope obtained for the test specimens sheared under undrained conditions. Similar curved envelopes for strength at low stress levels were recently noted by Parry and Nadarajah (1974).

Figure 10 illustrates the effective stress paths in a (q, p) plot for specimens sheared from 103·5, 172·5, 207, 276, 345 and 414 kN/m^2 consolidation stresses. The end points are also shown. In almost all the tests the maximum effective stress ratio occurred at the same strain. The line OA passing through the origin in the (q, p) plot is the projection of the critical state

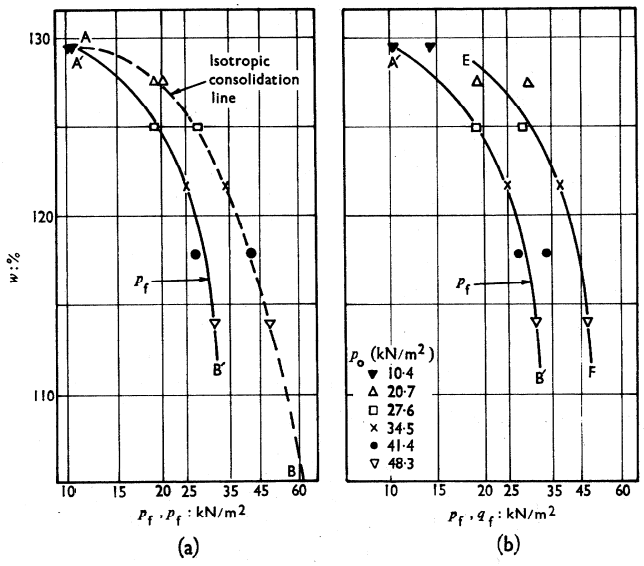

Fig. 11. (w_f, log p_f), (w_f, log q_f) relationships, $p_0 > 69$ kN/m^2

line. The slope of this line is expressed as M. The expression relating M to failure stresses is as follows:

$$q = Mp$$

M is found to be equal to 0·82, and the corresponding value of $\bar{\Phi}$ is 28·9°.

Water content shear strength relationships

The water content strength relationships for the test specimens are now presented for samples consolidated in the apparent overconsolidated state. In Fig. 11(a) the portion AB of the isotropic consolidation curve ABC has been plotted as broken lines. The full line A′B′ corresponds to the (w_f, log p_f) relationship. Thus the (w_f, log p_f) relationship is found to be approximately parallel to the (w, log p) relationship during isotropic consolidation. The end points of the specimens are thus found to lie on a Hvorslev type surface (see James and Balasubramaniam, 1971a and b). The (w_f, log q_f) relationship is shown in Fig. 11(b).

The water content shear strength relationships for normally consolidated specimens in test series CIUE-I are shown in Figs 12(a) and (b). In Fig. 12(a), the curve BC, plotted in broken lines corresponds to the virgin consolidation line. The (w_f, log p_f) relationship is shown by the full line B′C′ and is found to be a straight line parallel to the virgin consolidation line. The (w_f, p_f, q_f) relationship for normally consolidated samples as found by the authors is in full agreement with the finding of Roscoe *et al.* (1958), Henkel (1959) and James and Balasubramaniam (1971a and b).

TEST SERIES CIUE-II

In this series of tests 5 specimens were sheared under undrained extension condition. The samples were isotropically consolidated to pre-shear consolidation pressures of 10·4, 20·7, 27·6, 41·4 and 48·3 kN/m^2 and were then sheared under strain controlled condition. For this series of tests the axial stress of the specimen was kept constant, while the lateral stress was increased. In most of the figures associated with this test series, the results of the CIUE-I series of tests

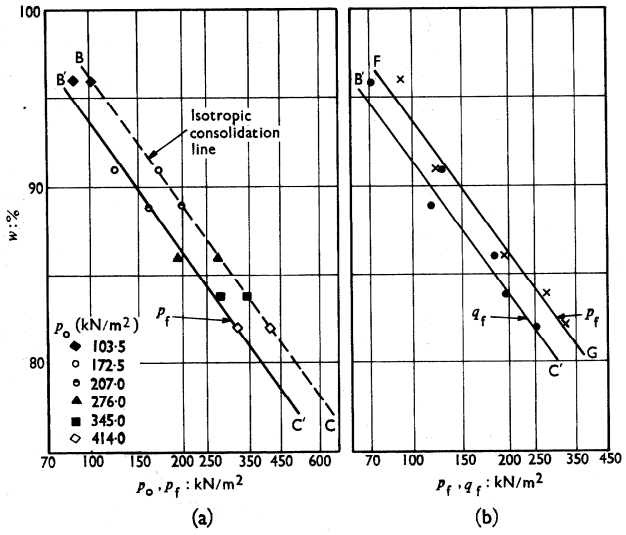

Fig. 12. (w_f, log p_f), (w_f log q_f) relationships, $p_o > 69$ kN/m²

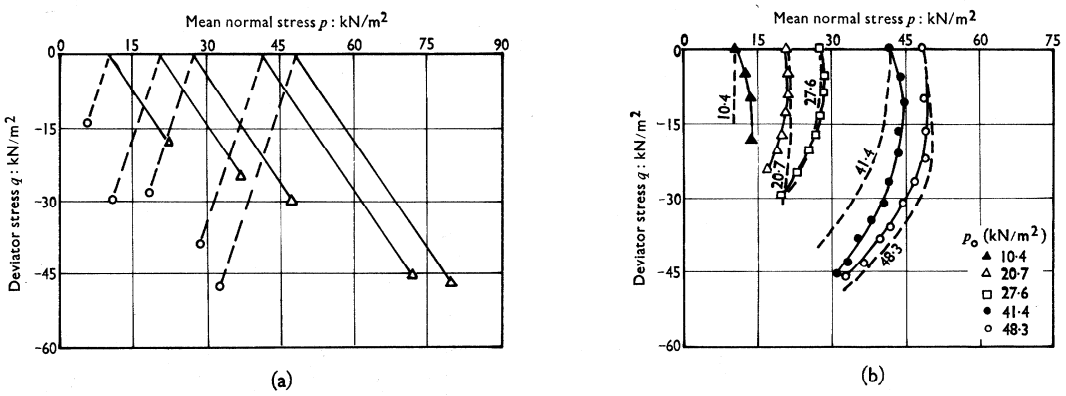

Fig. 13. (a) Applied stress paths for specimens in Series CIUE-II tests; (b) effective stress paths for specimens in Series CIUE-II tests

are shown by dashed lines. This would help in making a comparison of the behaviour under loading and unloading conditions.

Stress paths

The total and effective stress paths followed by these specimens are shown in Figs 13(a) and (b). The end points of the specimens are also shown in these figures. The effective stress paths are found to be convex towards the origin and are similar to the effective stress paths exhibited by lightly overconsolidated specimens. In all the specimens positive pore pressures developed during shear, and the effect of these positive pore water pressures would be to decrease the mean normal stress.

Figures 14(a) and (b) show the normalized effective stress paths for all the specimens in a (q/p_o, p/p_o) plot, where p_o is the pre-shear consolidation pressure. No unique curve exists for these specimens in the normalized plot. The shape of the normalized effective stress paths are dependent on the pre-shear consolidation pressure.

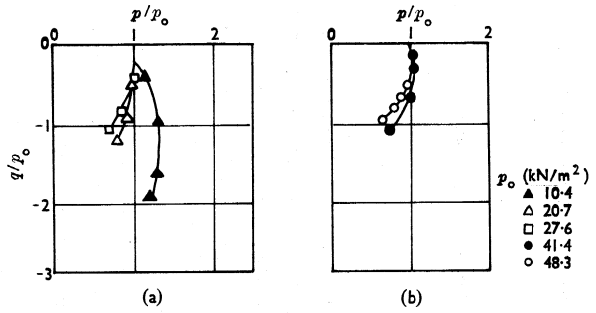

Fig. 14. Normalized effective stress paths (Series CIUE-II tests)

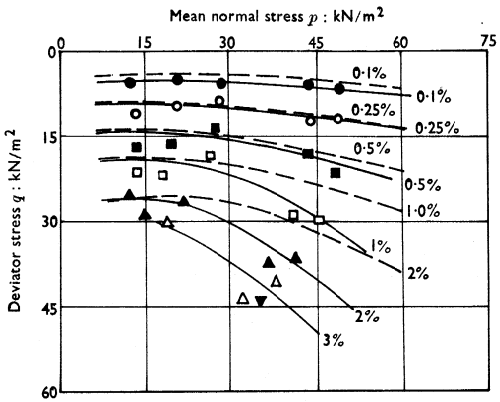

Fig. 15. Constant shear strain contours (Series CIUE-II tests)

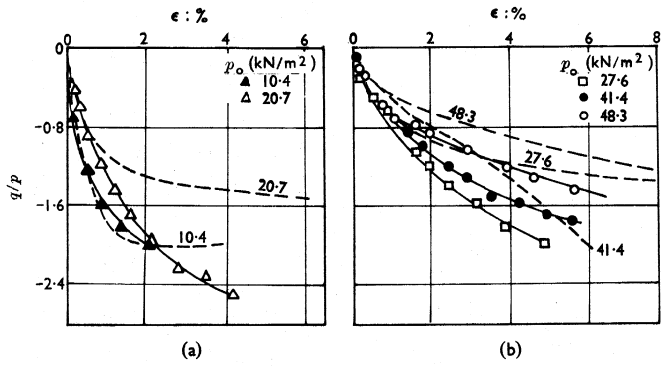

Fig. 16. Stress ratio–shear strain relationship (Series CIUE-II tests)

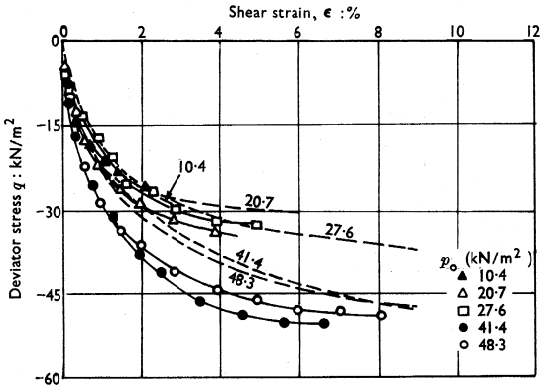

Fig. 17. Deviator stress–shear strain relationship for specimens sheared in Series CIUE-II tests

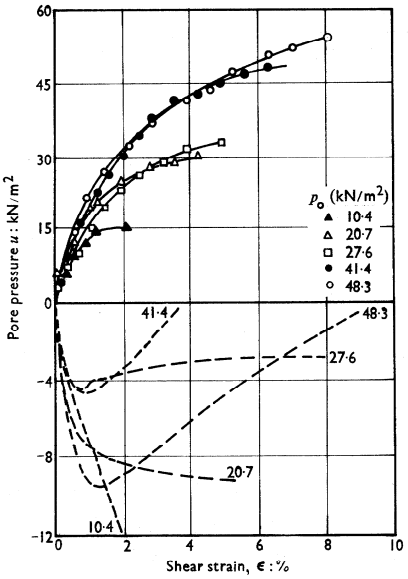

Fig. 18. Pore pressure–shear strain relationship (Series CIUE-II tests)

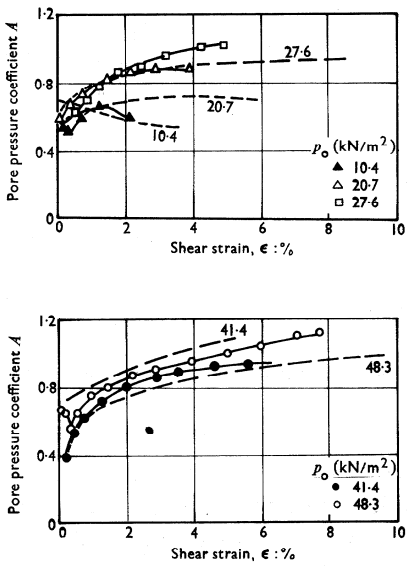

Fig. 19. Pore pressure coefficient–shear strain relationship (Series CIUE-II tests)

Shear strain contours

The constant shear strain contours have been superimposed in the effective stress paths in the (q, p) plot as shown in Fig. 15. The shear strain contours do not pass through the origin. It is noted that the trend shown by these contours is very similar to that shown in Fig. 4(a) by the constant shear strain contours of the CIUE-I Series of tests. At low strain levels the shear strain contours are slightly curved; however, they become more concave towards the p-axis as one moves from low to high consolidation pressures. But the contours are nearly parallel to each other. It shows that the shear strain at low levels largely depends on the deviator stress rather than the effective mean normal stress. This finding is similar to that discussed earlier for the unloading tests. At relatively higher strains, the shear strain contours become more curved and are concave towards the p-axis.

Stress ratio–shear strain relationships

For normally consolidated clays, the $(q/p, \epsilon)$ relationship is generally found to be unique and independent of the pre-shear consolidation pressures of the samples. Similar unique relationship was established by the Authors for weathered Bangkok Clay when consolidated to pressures which were high enough to transform the specimens from overconsolidated to the normally consolidated state. The $(q/p, \epsilon)$ relationships for all the tests in Series CIUE-II are shown in Figs 16(a) and (b). Here again the $(q/p, \epsilon)$ relationships are found to be dependent on the pre-shear consolidation pressures.

Deviator stress–shear strain relationships

The (q, ϵ) relationships of the specimens sheared from pre-shear consolidation pressures of 10·4, 20·7, 27·6, 41·4 and 48·3 kN/m² are shown in Fig. 17. In this figure, for each specimen the modulus of the deviator stress is found to increase with increase in magnitude of shear strain. At any particular strain, the moduli of the deviator stresses are found to be proportional to the magnitude of the pre-shear consolidation pressure.

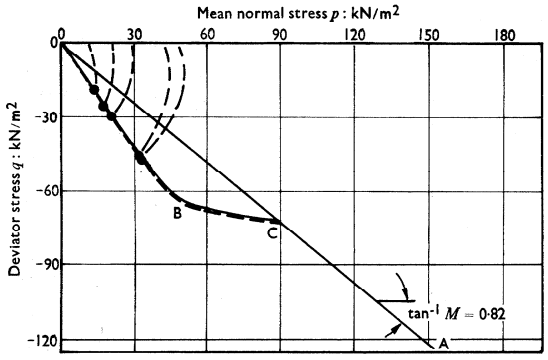

Fig. 20. End points of specimens in (q, p) plot (Series CIUE-II tests)

However, for the specimens sheared from 41·4 and 48·3 kN/m^2 the (q, ϵ) relationships are found to be approximately the same. Similarly for the specimens sheared from 10·4, 20·7 and 27·6 kN/m^2, the (q, ϵ) relationships are again found to be approximately the same.

Excess pore pressure–shear strain relationships

The excess pore pressure–shear strain relationships for the specimens are shown in Fig. 18. It is interesting to note that the pore pressure–shear strain relationships for the specimens sheared from 41·4 and 48·3 kN/m^2 are virtually the same. For these specimens, the (q, ϵ) relationship was also found to be independent of the pre-shear consolidation pressure. The pore pressure–shear strain relationships for specimens sheared from isotropic stresses of 20·7 and 27·6 kN/m^2 are also unique. But these relationships are somewhat different from those of the specimens sheared from isotropic stresses of 41·4 and 48·3 kN/m^2. The specimen sheared from an isotropic stress of 10·4 kN/m^2 has a pore pressure–shear strain relationship which corresponds to the lowest pore pressure when compared with the rest of the specimens.

Pore pressure coefficient A against shear strain relationships

Figure 19 illustrates the pore pressure coefficient A against shear strain relationships for all the samples tested in series CIUE-II. It is seen that (A, ϵ) relationship is rather dependent on pre-shear consolidation pressure. Initially, the value of A lies at about 0·6 for the samples tested from 10·4, 20·7, 27·6 and 48·3 kN/m^2 consolidation pressure. The initial value of A is about 0·4 for the sample tested from 41·4 kN/m^2 consolidation pressure. It is noted that the value of A remains considerably low for the sample of 10·4 kN/m^2 in comparison to all other tests at any particular shear strain. Value of A at failure is lowest for the sample at the lowest consolidation pressure.

Shear strength characteristics

Figure 20 illustrates the failure envelope OBC found by the Authors from all the tests in Series CIUE-II. The effective stress paths are also shown in this plot. The end points were selected with respect to the maximum stress ratio criterion. The line OA corresponds to the projection of the critical state line as obtained from CIUE-I series of tests. The full line OBC corresponds to the failure envelope obtained from the tests carried out in Series CIUE-II under undrained loading condition. This curved failure envelope is similar to that (shown by dashed lines) found by the Authors in the apparent overconsolidated state from test series CIUE-I.

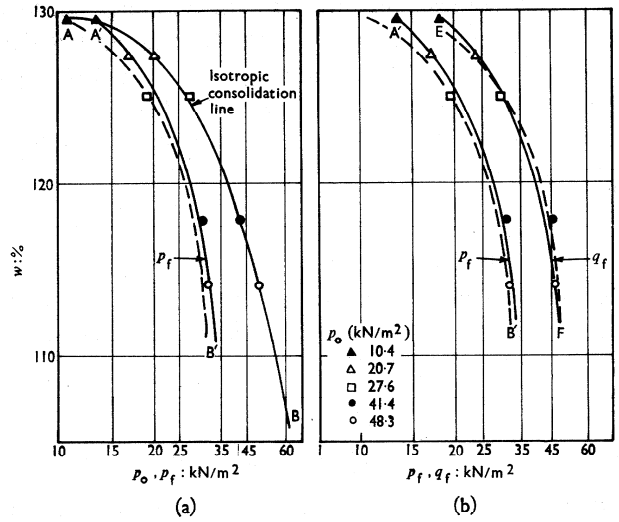

Fig. 21. **(w, log p_f), (w_f, log q_f) relationship for specimens sheared in Series CIUE-II tests**

The (w_f, log p_f) and the (w_f, log q_f) relationships are shown in Figs 21(a) and (b). These relationships are similar to those presented for CIUE-I series of tests.

CONCLUSIONS

The deformation characteristics of weathered Bangkok Clay is studied in detail by carrying out two series of strain controlled undrained triaxial tests under extension condition.

Series I corresponded to the case when the axial stress was reduced and the lateral stress was maintained constant. From these tests the following conclusions are reached:

(*a*) For pre-shear consolidation pressures less than the critical pressure

- (*i*) the undrained effective stress paths, the pore pressure coefficient A, and the normalized stress–strain behaviour are dependent on the pre-shear consolidation pressures
- (*ii*) the constant shear strain contours in (q, p) plot are such that at lower strains, the magnitude is largely dependent on the increment of deviator stress, rather than any change in the mean normal stress
- (*iii*) the failure envelope in (q, p) plot is found to be curved with appreciable cohesion. The relationship between water content and the stresses p and q are found to be parallel to the isotropic consolidation line in a semi-log plot.

(*b*) For pre-shear consolidation pressures higher than the critical pressure

- (*i*) the undrained effective stress paths are geometrically similar
- (*ii*) the normalized stress–strain behaviour is independent of the pre-shear consolidation pressure
- (*iii*) the shear strain is uniquely dependent on the stress-ratio
- (*iv*) the failure envelope is a straight line in the (q, p) plot and is found to pass through the origin. The relationships between the water content and the stress p and q are found to be linear in semi-log plots and are parallel to the isotropic consolidation line.

Series II tests corresponded to the case when the axial stress was kept constant and the lateral stress was increased. Here again the effective stress paths and the normalized stress–strain behaviour were found to be dependent on the pre-shear consolidation pressure. Also, the effective stress paths, the constant shear strain contours and the failure envelopes from these tests were also found to be very similar to those obtained in Series I tests for pre-shear consolidation pressures less than the maximum past pressure.

ACKNOWLEDGEMENTS

The work presented in this Paper was carried out at the Asian Institute of Technology. Thanks are due to Messrs Ruangvit Chotivittayathanin and Suvit Viranuvut for their assistance in carrying out the experimental programme. Thanks are also due to Professors Za-Chieh Moh, Edward W. Brand and Mrs Vatinee Chern.

REFERENCES

Balasubramaniam, A. S. (1973). Stress history effects on the stress–strain behaviour of a saturated clay. *Geotch. Engng J.* **4**, 91–111.

Balasubramaniam, A. S. (1974). A critical study of the uniqueness of state boundary surface for saturated specimens of kaolin. *Geotech. Engng*, Journal of Southeast Asian Society of Soil Engineering **V**, No. 1, 21–38.

Chang, R. T. (1974). *Shear strength characteristics of weathered Nong Ngoo Hao Clay under isotropically consolidated undrained compression test.* M.Eng. Thesis, Asian Institute of Technology, Bangkok.

Henkel, D. J. (1959). The relationship between strength, pore water pressure and volume change characteristics of saturated clays. *Géotechnique* **9**, No. 3, 119–135.

James, R. G. & Balasubramaniam, A. S. (1971a). The peak stress envelopes and their relation to the critical state line for a saturated clay. *Proc. 4th Asian Regional Conf. Soil Mech. and Found. Engng*, Bankgkok, 115–120.

James, R. G. & Balasubramaniam, A. S. (1971b). A comprehensive experimental study of the strength characteristics of remoulded specimens of kaolin. *Geotech. Engng*, Journal of Southeast Asian Society of Soil Engineering **II**, No. 1, 21–23.

Moh, Z. C., Nelson, J. D. & Brand, E. W. (1969). Strength and deformation behaviour of Bangkok Clay. *Proc. 7th Int. Conf. Soil Mechs Found. Engng, Mexico* **1**, 287–295.

Muktabhant, C., Teerawong, P. & Tengamnuay, V. (1967). *Engineering properties of Bangkok subsoils.* Chulalongkorn University Report, Bangkok.

Parry, R. H. G. (1960). Triaxial compression and extension tests on remoulded saturated clay. *Géotechnique* **10**, No. 4, 166–180.

Parry, R. H. G. & Nadarajah (1974). Observations on laboratory prepared lightly overconsolidated specimens of kaolin. *Géotechnique* **24**, No. 3, 345–350.

Roscoe, K. H. & Burland, J. B. (1968). On the generalized stress–strain behaviour of wet clay. *Engng Plast.* Cambridge University Press, 535–609.

Roscoe, K. H. & Poorooshasb, H. B. (1963). A theoretical and experimental study of strains in triaxial tests on normally consolidated clays. *Géotechnique* **13**, No. 1, 12–38.

Roscoe, K. H., Schofield, A. N. & Thurairajah, A. (1963). Yielding of clays in states wetter than critical. *Géotechnique* **13**, No. 3, 211–240.

Roscoe, K. H., Schofield, A. N. & Wroth, C. P. (1958). On the yielding of Soils. *Géotechnique* **8**, No. 1, 22–53.

Schofield, A. N. & Wroth, C. P. (1968). *Critical state soil mechanics.* London: McGraw-Hill.

Shibata, T. & Karube, D. (1965). Influence of the variation of intermediate principal stress on the mechanical properties of normally consolidated clays. *Proc. 6th Int. Conf. Soil Mechs Found. Engng*, Montreal **1**, 359–363.

Vaid, Y. P. & Campanella, R. G. (1974). Triaxial and plane strain behaviour of a natural clay. *J. Geotech. Engng Div., ASCE* **100**, GT 3, 207–223.

Wang, C. H. (1974). *Undrained shear strength characteristics of Nong Ngoo Hao weathered clay under K_0 conditions.* M.Eng. Thesis, Asian Institute of Technology, Bangkok.

Wroth, C. P. & Loudon, P. A. (1967). The correlation of strains within a family of triaxial tests on overconsolidated samples of kaolin. *Proc. Geotech. Conf. Shear Strength of Soils, Oslo* **1**, 159–163.

Wu, T. H., Loh, A. K. & Malvern, L. E. (1963). Study of failure envelopes of soils. *J. Soil Mech. Fdn. Div., ASCE* **80**, SM3, 145–181.